Inorganic Chemistry
Article
Cite This: Inorg. Chem. 2018, 57, 12876−12884
pubs.acs.org/IC

Using Diamagnetic Yttrium and Lanthanum Complexes to Explore Ligand Reduction and C−H Bond Activation in a Tris(aryloxide)mesitylene Ligand System

Chad T. Palumbo,[†] Dominik P. Halter,[‡] Vamsee K. Voora,[†] Guo P. Chen,[†] Joseph W. Ziller,[†] Milan Gembicky,[§] Arnold L. Rheingold,[§] Filipp Furche,*[,†] Karsten Meyer,*[,‡] and William J. Evans*[,†]

[†]Department of Chemistry, University of California, Irvine, California 92697-2025, United States
[‡]Department of Chemistry and Pharmacy, Inorganic Chemistry, Friedrich-Alexander-University Erlangen-Nürnberg, Egerlandstrasse 1, D-91058 Erlangen, Germany
[§]Department of Chemistry and Biochemistry, University of California, San Diego, 9500 Gilman Drive, MC 0332, La Jolla, California 92093, United States

Supporting Information

ABSTRACT: $[Y(N(SiMe_3)_2)_3]$ reacts with $(^{Ad,Me}ArOH)_3mes$ to form the Y^{3+} complex $[((^{Ad,Me}ArO)_3mes)Y]$, **1-Y**. This complex reacts with potassium metal in the presence of 2.2.2-cryptand to give a cocrystallized mixture of $[K(2.2.2\text{-cryptand})][((^{Ad,Me}ArO)_3mes)Y]$, **2-Y**, and $[K(2.2.2\text{-cryptand})][((^{Ad,Me}ArO)_3mes)YH]$, **3-Y**. The electron paramagnetic resonance spectrum of this crystalline mixture exhibits an isotropic signal at 77 K (g_{iso} = 2.000, W_{iso} = 1.8 mT), suggesting that **2-Y** is best described as a Y^{3+} complex of the tris(aryloxide)mesitylene radical $((^{Ad,Me}ArO)_3mes)^{4-}$. Evidence of the hydride ligand in **3-Y** was obtained by $^{89}Y-^{1}H$ heteronuclear multiple quantum coherence NMR spectroscopy, and a coupling constant of J_{YH} = 93 Hz was observed. A single crystal of **3-Y** was also obtained in pure form and structurally characterized for comparison with the crystal data on the mixed component **2-Ln**/**3-Ln** crystals. The origin of the hydride in **3-Ln** is unknown, but further studies of the reduction of **1-La**, previously found to form **2-La**, revealed a possible source. Ligand-based C−H bond activation and loss of hydrogen can occur under reducing conditions to form a tetraanionic ligand derived from $((^{Ad,Me}ArO)_3mes)^{3-}$, as observed in $[K(2.2.2\text{-cryptand})][((^{Ad,Me}ArO)_3(C_6Me_3(CH_2)_2CH)La]$, **4-La**.

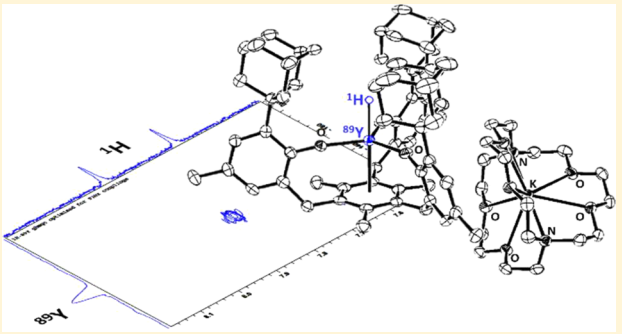

INTRODUCTION

Recent studies of reductive f-element chemistry have involved comparisons of the tris(cyclopentadienyl) ligand sets $(Cp'_3)^{3-}$ and $(Cp''_3)^{3-}$ ($Cp' = C_5H_4SiMe_3$; $Cp'' = C_5H_3(SiMe_3)_2$)[1−10] with the tris(aryloxide)mesitylene ligand $((^{Ad,Me}ArO)_3mes)^{3-}$.[11−14] Reduction of the tris(cyclopentadienyl) complexes Cp'_3M and Cp''_3M has allowed the isolation of M^{2+} complexes for Y, all the lanthanides (except *Pm*), Th, U, Pu, and Np as shown in eq 1.[1−10] New Ln^{2+} ions are also known with two $C_5H_3(CMe_3)_2$[15] (Cp^{tt}) and $C_5H_2(CMe_3)_3$[16,17] (Cp^{ttt}) ligands.

Reduction of the tris(aryloxide)mesitylene complexes, $[((^{Ad,Me}ArO)_3mes)U]$, **1-U**, and $[((^{Ad,Me}ArO)_3mes)Ln]$, **1-Ln**, has been used to generate M^{2+} complexes of U, Nd, Sm, and Yb, eq 2.[13,14]

However, reduction of the **1-Ln** complexes of Gd, Dy, and Er was more complicated.[13] In each case, a mixture of a Ln^{2+} complex, $[K(2.2.2\text{-cryptand})][((^{Ad,Me}ArO)_3mes)Ln]$, **2-Ln**, and a Ln^{3+} hydride product, $[K(2.2.2\text{-cryptand})][((^{Ad,Me}ArO)_3mes)LnH]$, **3-Ln**, was obtained as a cocrystallized material, eq 3. The source of the hydride is unknown.

Reduction of **1-Ln** with Ln = La, Ce, or Pr gave yet another result: the products are best described as Ln^{3+} complexes of a reduced $((^{Ad,Me}ArO)_3mes)^{4-}$ ligand radical, eq 4.[14]

To obtain more information on the reductive chemistry of this flexible tris(aryloxide)mesitylene ligand system, studies have now been extended to yttrium, since the ^{89}Y isotope (100% natural abundance) has an $I = 1/2$ nuclear spin that can provide additional information via NMR and electron paramagnetic resonance (EPR) spectroscopy for Y^{3+} and Y^{2+} complexes, respectively. Historically, Y^{3+} has been shown to display chemistry similar to the late lanthanides of similar size, for example, Ho^{3+} and Er^{3+}.[18,19] This has been very helpful in elucidating the chemistry of these highly paramagnetic ions that are difficult to study by NMR spectroscopy. We also

Received: July 24, 2018
Published: September 24, 2018

DOI: 10.1021/acs.inorgchem.8b02053
Inorg. Chem. 2018, 57, 12876−12884

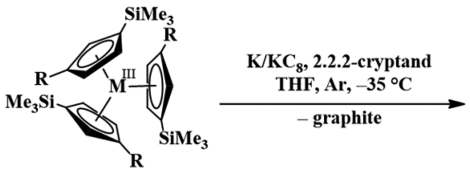

R = $SiMe_3$; M = La, Th, U, Np, Pu
R = H; M = Y, La, Ce, Pr, Nd, Sm, Gd, Tb, Dy, Ho, Er, Tm, Lu, U

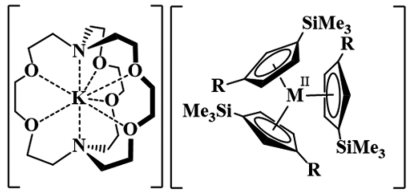

(1)

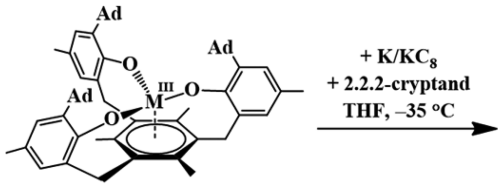

1-M

(2)

2-M
M = U, Nd, Sm, Yb

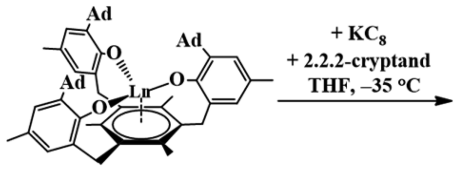

1-Ln

Ln = Gd; x = 0.65, y = 0.35
Ln = Dy; x = 0.63, y = 0.37
Ln = Er; x = 0.55, y = 0.45

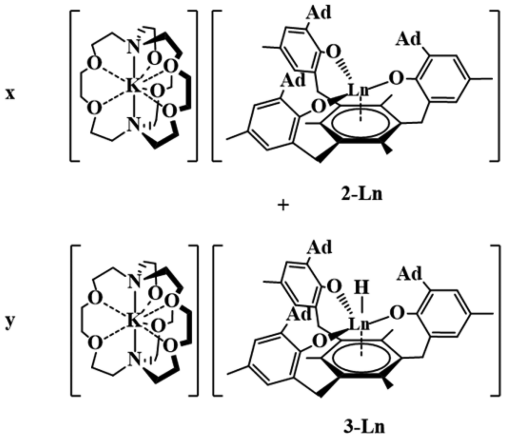

2-Ln

(3)

3-Ln

explored further the reduction of the diamagnetic La^{3+} complex [((^{Ad,Me}ArO)$_3$mes)La], **1-La**,[14] since it is a congener of yttrium, and have found a new product in addition to **2-La** in eq 4 that could explain the source of the hydride ligands in eq 3.

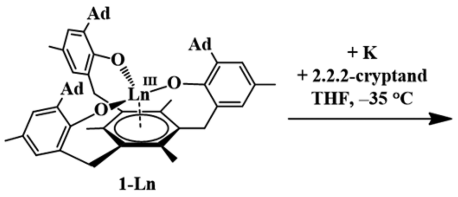

1-Ln

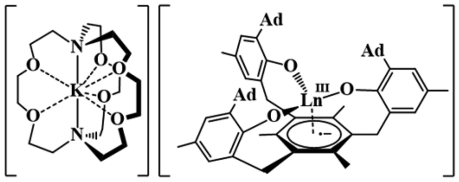

(4)

2-Ln
Ln = La, Ce, Pr

RESULTS

Protonolysis of the tris(amide) compound [Y(N(SiMe$_3$)$_2$)$_3$][20] with the tris(phenol) (^{Ad,Me}ArOH)$_3$mes[12] gave colorless solids whose composition was determined to be [((^{Ad,Me}ArO)$_3$mes)-Y], **1-Y**, by X-ray crystallography, Figure 1. The structure features metrical parameters that are intermediate between those of **1-Dy** and **1-Er**,[13] Table 1. This is consistent with the similar ionic radii of these three metals.

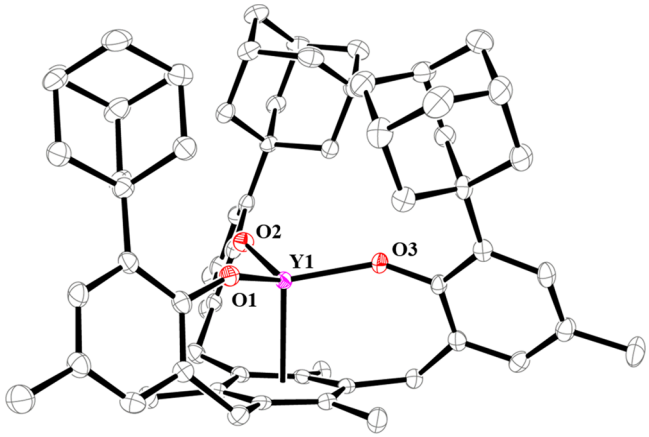

Figure 1. Molecular structure of [((^{Ad,Me}ArO)$_3$mes)Y], **1-Y**, with thermal ellipsoids drawn at the 50% probability level. Hydrogen atoms are omitted.

Treatment of a colorless tetrahydrofuran (THF) solution of **1-Y** with potassium metal in the presence of 2.2.2-cryptand generated a dark red solution reminiscent of the color of the **1-Ln** reductions in eqs 2–4. Diffusion of Et_2O into the dark red THF solution at −35 °C similarly gave crystals, which were identified as the cocrystallized mixture, [K(2.2.2-cryptand)]-[((^{Ad,Me}ArO)$_3$mes)Y]/[K(2.2.2-cryptand)][((^{Ad,Me}ArO)$_3$mes)-YH], **2-Y**/**3-Y**, Figure 2, in a reaction analogous to that of eq 3. **2-Y**/**3-Y** crystallizes in the space group $P2_13$ and is isomorphous with the previously reported **2-Ln**/**3-Ln** analogues of Gd, Dy, and Er that also cocrystallize as mixtures. The data were best refined as a 47:53 mixture of **2-Y**/**3-Y**. For

DOI: 10.1021/acs.inorgchem.8b02053
Inorg. Chem. 2018, 57, 12876–12884

Table 1. Selected Bond Lengths (Å) and Angles (deg) of 1-Y and 1-Ln (Ln = Dy, Er)[13] Complexes Listed in Order of Decreasing Ionic Radius

metal	ionic radius for coordination number 6[a]	M−O range	M−O avg	M−C_6 (ring centroid)	M out of plane[b]	C_6 torsion angle[c]
Dy[13]	0.912	2.093(3)-2.095(3)	2.094(1)	2.368	0.443	8.1
Y	0.90	2.085(2)-2.088(2)	2.087(1)	2.368	0.445	9.6
Er[13]	0.89	2.078(2)-2.081(2)	2.079(1)	2.336	0.477	7.9

[a]According to the values by Shannon.[21] [b]Distance of M from the plane defined by the three O atoms of the $((^{Ad,Me}ArO)_3mes)^{3-}$ ligand. [c]The largest dihedral angle between adjacent three carbon plane in the mesitylene ring.

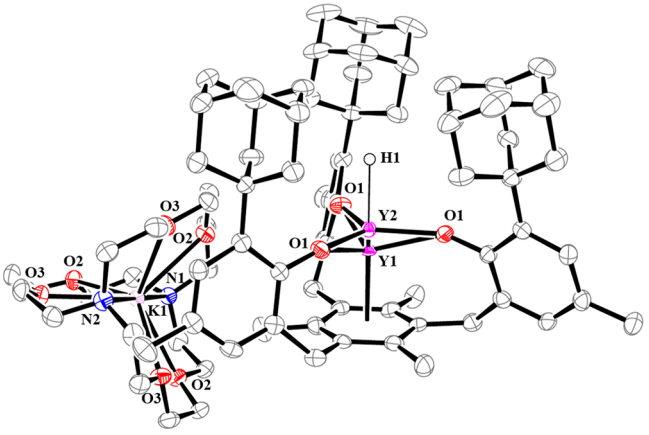

Figure 2. Molecular structure of [K(2.2.2-cryptand)][$((^{Ad,Me}ArO)_3mes)$Y]/[K(2.2.2-cryptand)][$((^{Ad,Me}ArO)_3mes)$YH], **2-Y/3-Y**, with thermal ellipsoids drawn at the 50% probability level. Hydrogen atoms except H1 attached to Y2 in **3-Y** are omitted.

comparison, the distributions for Gd, Er, and Dy were 65:35, 55:45, and 63:37, respectively.[13]

In one reduction reaction, crystals of pure **3-Y** were obtained (see Figure S3 in the Supporting Information). This is the first pure tris(aryloxide)mesitylene rare-earth metal hydride complex isolated. Attempts to make this complex independently were not successful, but the crystals of **3-Y** show the variation in metrical parameters that can occur between crystal data of the pure hydride, **3-Y**, and the **3-Y** component in the **2-Y/3-Y** crystal. For example, the Y−O_{Ar} and Y−(arene ring centroid) distances in pure **3-Y** were measured to be 2.135(3) and 2.775 Å, but in the **2-Y/3-Y** mixture, the model showed these distances to be 2.095(2) and 2.822 Å. For this reason, the data on the cocrystallized mixtures were not used to rationalize bonding. The bond distances and angles of **3-Ln** in the **2-Ln/3-Ln** structures (Table S2) and the differences between **2-Y** and **1-Y** (Table S3) are given in the Supporting Information along with all the other lanthanide examples.

Although the ^{1}H NMR spectrum generated from the crystals of **2-Y/3-Y** in deuterated tetrahydrofuran (THF-d_8) is complicated, the resonance of the hydride ligand could be identified as a doublet centered at 7.81 ppm. The J_{YH} = 93 Hz coupling constant is larger than, but consistent with, the J_{YH} = 74.8, 81.7, and 82.0 Hz coupling constants reported for the terminal hydride complexes $[(C_5Me_4SiMe_3)_2YH(THF)]$,[22] $[(C_5Me_5)_2YH(THF)]$,[23] and $[(C_9Me_7)_2YH(THF)]$,[24] respectively. In contrast, for μ_2-hydride complexes, J_{YH} coupling constants have been reported in the range of 21.3−35 Hz.[25−42] The J_{YH} coupling constants for μ_3-hydrides are 16.3−18 Hz,[43−45] and they are 12.5 and 15.3 Hz for μ_4-hydrides.[25,46] A ^{89}Y−^{1}H heteronuclear multiple quantum coherence (HMQC) experiment showed a correlation between the hydride resonance at 7.81 ppm with a ^{89}Y resonance at −138.0 ppm in the ^{89}Y NMR spectrum of **2-Y/3-Y**. When CCl_4 is added to

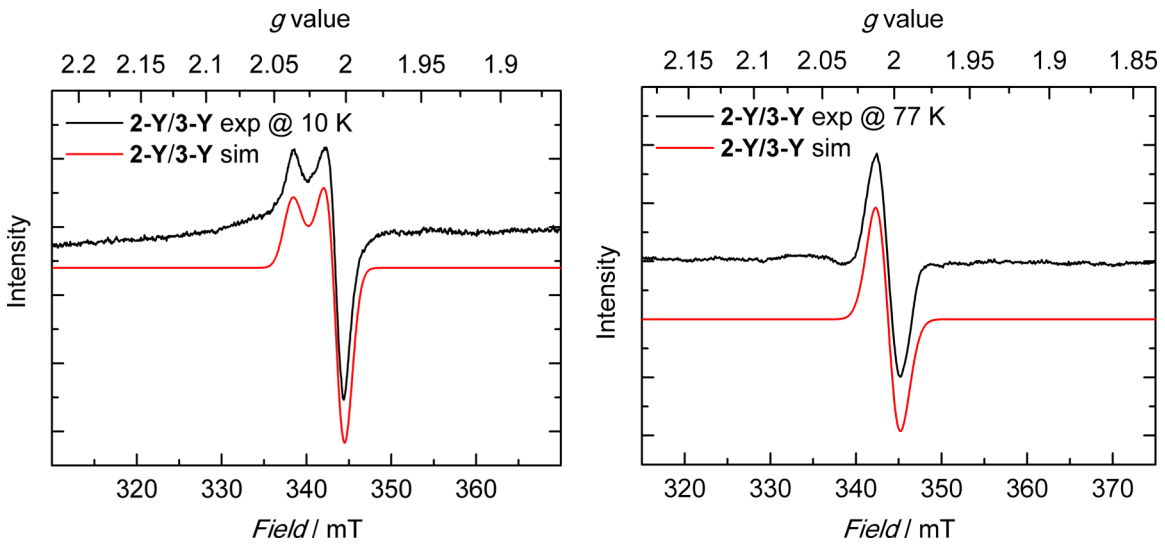

Figure 3. (left) Experimental X-band EPR spectrum (black trace) of a frozen solution of single crystals of **2-Y/3-Y** dissolved in THF (1 mM) at 10 K (mode: perpendicular; ν = 9.643 GHz; P = 6.408 mW; modulation amplitude = 10.02 G). The best fit (red trace) was obtained for an axial symmetric spectrum with g_{par} = 2.036, g_{per} = 2.003, W_{par} = 1.2 mT, and W_{per} = 1.3 mT. (right) Experimental X-band EPR spectrum (black trace) of a frozen solution of single crystals of **2-Y/3-Y** dissolved in THF (1 mM) at 77 K (mode: perpendicular; ν = 9.627 GHz; P = 6.408 mW; modulation amplitude = 10.02 G). The best fit (red trace) was obtained for an isotropic spectrum with g_{iso} = 2.000, W_{iso} = 1.7 mT. The 77 K spectrum was corrected for the background signal generated from the cavity (see Figure S6 in the Supporting Information).

DOI: 10.1021/acs.inorgchem.8b02053
Inorg. Chem. 2018, 57, 12876−12884

the NMR sample, the 7.81 ppm resonance disappears, and chloroform at 7.89 ppm grows in, which is consistent with the presence of a hydride ligand.[47] These spectra can be found in the Supporting Information (Figure S7).

The EPR spectrum at 10 K of a frozen THF solution prepared by dissolving crystals of the **2-Y**/**3-Y** mixture showed an axial symmetric signal with g values at g_{par} = 2.036 and g_{per} = 2.003, Figure 3. A similar spectrum was observed for the previously reported **2-La**[14] at 10 K (see Figure S5 in the Supporting Information). At 77 K, the frozen solution gives an apparent isotropic singlet centered at g_{iso} = 2.000.

This is consistent with an organic radical rather than a Y^{2+} compound. Complexes of $4d^1$ Y^{2+} typically display two line patterns in their EPR spectra with g = 1.976−1.986 and hyperfine coupling constants A = 34.6−46.9 G in tris(cyclopentadienyl) compounds[48−50] and A = 110 G in reduction reactions of the tris(amide) yttrium complex, $[Y(N(SiMe_3)_2)_3]$.[51] Hence, the **2-Y** component in the **2-Y**/**3-Y** crystal appears to contain Y^{3+} with an $((^{Ad,Me}ArO)_3mes)^{4-}$ radical ligand. In this regard, **2-Y** is like congeneric **2-La**, along with **2-Ce** and **2-Pr**, which were also characterized as Ln^{3+} complexes with $[(^{Ad,Me}ArO)_3mes]^{4-}$ radical ligands.[14] The EPR spectrum of **2-La** under analogous conditions (Figure S5 in the Supporting Information) appears nearly identical to those of the **2-Y**/**3-Y** crystals.

Computational studies on the anion in **2-Y**, $[((^{Ad,Me}ArO)_3mes)Y]^{1-}$, using the Tao-Perdew-Staroverov-Scuseria (TPSS)[52] density functional approximation, support the assignment made from the EPR data. The highest occupied molecular orbital (HOMO) is predominantly localized on the mesitylene ring, Figure 4. The Mulliken population analysis using spin density difference shows that ∼0.8 excess negative charge is located on the ligand, which indicates mesitylene-ring reduction.

Given the useful results obtained by examining diamagnetic **1-Y**, further studies of the reduction of diamagnetic **1-La** were conducted. In addition to the red **2-La** product isolated in eq 4,[14] a low-yield coproduct was isolated as a bright orange solid that precipitated out of solution during the crystallization of **2-La**. The material could be recrystallized to give red microcrystals identified by X-ray crystallography as a complex that has lost hydrogen from a methylene group on the mesitylene component of the ligand: [K(2.2.2-cryptand)]-$[((^{Ad,Me}ArO)_3(C_6Me_3(CH_2)_2CH)La]$, **4-La**, Figure 5. Previously, a U^{4+} hydride complex of this $((^{Ad,Me}ArO)_3(C_6Me_3(CH_2)_2CH))^{4-}$ ligand, namely, $[((^{Ad,Me}ArO)_3(C_6Me_3(CH_2)_2CH))U(\mu\text{-}H)K(Et_2O)]$, **5-U**, had been isolated from the reaction of **1-U** with KC_8 or Na in benzene.[12] The two complexes share many similarities, and their structural parameters are compared in Table 2.

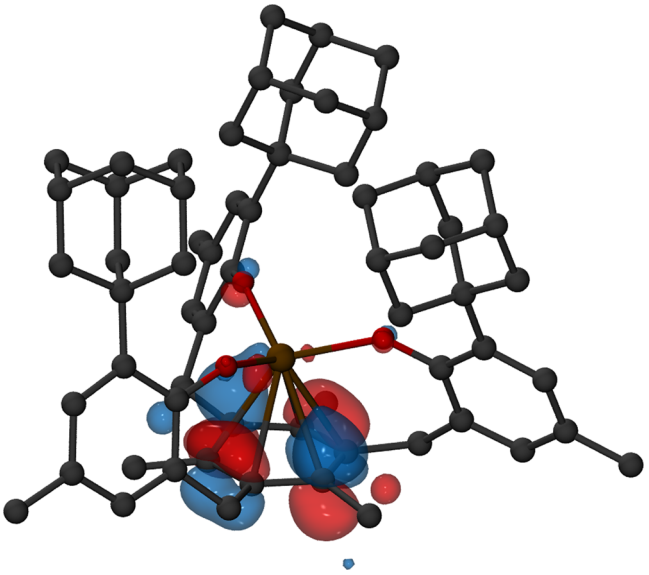

Figure 4. Isosurfaces for the highest singly occupied orbital of **2-Y** corresponding to a contour value of 0.05. Hydrogen atoms are omitted.

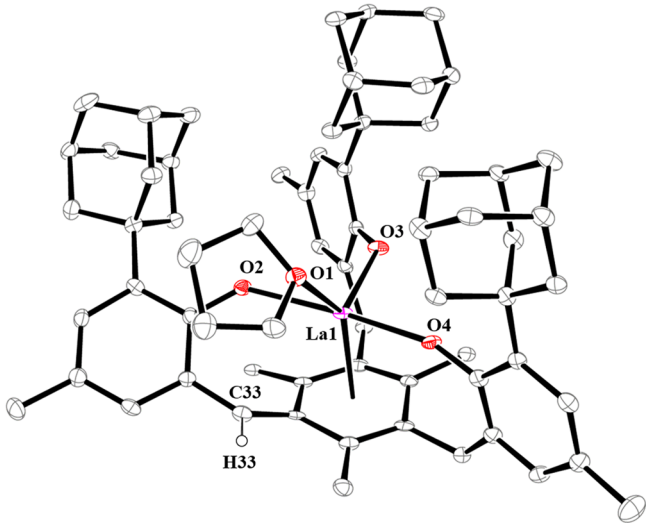

Figure 5. Molecular structure of the anion of [K(2.2.2-cryptand)]-$[((^{Ad,Me}ArO)_3(C_6Me_3(CH_2)_2CH))La(THF)]$, **4-La**, with thermal ellipsoids drawn at the 50% probability level. The methine atoms are labeled as C33 and H33. All other hydrogen atoms and a $[K(2.2.2\text{-cryptand})]^+$ cation are omitted.

Both **4-La** and **5-U** have three rather different $M-O_{OAr}$ distances that deviate by up to 0.1 Å. The distances in **4-La** differ from those in **5-U**, because the Shannon ionic radius of seven-coordinate La^{3+} is 0.15 Å larger than that of U^{4+},[21] but the differences for all three distances are close to this 0.15 Å value. The distance of the metal out of the plane of the three aryloxide oxygen atoms is similar in the two complexes as is the largest torsional angle of the arene ring, which is a measure of its nonplanarity. In both complexes, the aryloxide arms of the ligand have undergone a T-shaped distortion that gives three different $O_{Ar}-La-O_{Ar}$ angles that are similar in **4-La** and **5-U**. Both complexes have one short $C_{arene}-C_{benzylic}$ bond distance consistent with a C=C double bond. The complexes differ in that **4-La** has one short La−C bond, 2.668(6) Å, while all the others are over 2.816(6) Å. In contrast, **5-U** has all the U−C bonds in the narrow range of 2.729(3)−2.766(3) Å.

TPSS-D3 calculations on **4-La** confirm the presence of the $((^{Ad,Me}ArO)_3(C_6Me_3(CH_2)_2CH))^{4-}$ ligand and show that the highest occupied molecular orbital (HOMO) is delocalized over the mesitylene and O2 aryloxide arm; see Figure 6. Further, the computed $C_{arene}-C_{benzylic}$ interatomic distances match the experimentally observed values within 0.01 Å; see Table S5 in the Supporting Information. This agreement confirms that the loss of a hydrogen atom occurs at the benzylic position of one of the aryloxide arms of the $((^{Ad,Me}ArO)_3mes)^{3-}$ ligand.

DOI: 10.1021/acs.inorgchem.8b02053
Inorg. Chem. 2018, 57, 12876−12884

Table 2. Selected Bond Lengths (Å) and Angles (deg) of [K(2.2.2-cryptand)][((^{Ad,Me}ArO)$_3$(C$_6$Me$_3$(CH$_2$)$_2$CH)La], 4-La, and [((^{Ad,Me}ArO)$_3$(C$_6$Me$_3$(CH$_2$)$_2$CH))U(μ-H)K(Et$_2$O)],[12] 5-U

	M−O	M−C	M out of O_3 plane[a]	C_{arene}−$C_{benzylic}$	O−M−O	largest C_6 torsion angle[b]
4-La	2.349(4)	2.668(6)	0.18	1.410(9)	90.56(15)	18.4
	2.288(4)	2.816(6)		1.524(9)	103.64(15)	
	2.392(4)	2.841(6)		1.530(9)	162.75(14)	
		2.852(6)				
		2.914(6)				
		2.984(6)				
5-U[12]	2.144(4)	2.729(3)	0.20	1.425(7)	83.20(13)	23.3
	2.181(3)	2.732(3)		1.508(7)	107.57(13)	
	2.232(3)	2.736(3)		1.523(8)	164.28(13)	
		2.754(3)				
		2.766(3)				
		2.774(3)				

[a]Distance of M from the plane defined by the three O atoms of the ((^{Ad,Me}ArO)$_3$mes)$^{3-}$ ligand. [b]The largest dihedral angle between adjacent three carbon planes in the mesitylene ring.

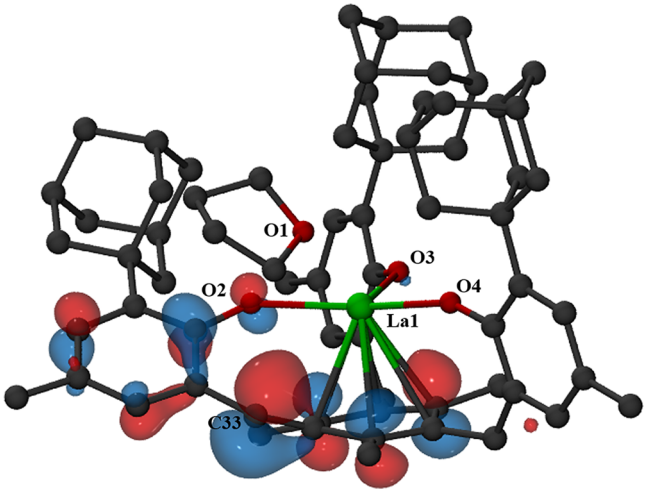

Figure 6. Isosurfaces for the HOMO of [K(2.2.2-cryptand)][((^{Ad,Me}ArO)$_3$(C$_6$Me$_3$(CH$_2$)$_2$CH))La(THF)], **4-La**, corresponding to a contour value of 0.05. The methine carbon is labeled as C33. Hydrogen atoms are omitted.

DISCUSSION

The extension of the ((^{Ad,Me}ArO)$_3$mes)$^{3-}$ ligand system to yttrium allowed the isolation and structural characterization of [(^{Ad,Me}ArO)$_3$mes)Y], **1-Y**, and its cocrystallized reduction products **2-Y** and **3-Y**, which are structurally analogous to those isolated for the late lanthanide series Gd, Dy, and Er. The diamagnetism of Y^{3+} and the I = 1/2 nuclear spin of its most abundant isotope has allowed the definitive identification of the hydride ligand by NMR spectroscopy. Evidence for the hydride ligand was also supported in the reactivity of the **2-Y**/**3-Y** crystal with CCl_4, which showed the disappearance of the hydride resonance and the appearance of the resonance for $CHCl_3$. The **2-Y** component of the **2-Y**/**3-Y** crystal is structurally similar to the **2-Ln** component of the previously reported **2-Ln**/**3-Ln** complexes of Ln = Gd, Dy, and Er,[13] in that the M−(arene ring centroid) distance decreases upon reduction of **1-Ln** and the M−O_{Ar} distances increase slightly. However, EPR spectroscopy and density functional theory (DFT) calculations suggest that **2-Y** is closer to its congener **2-La** and best described as a combination of Y^{3+} and a ((^{Ad,Me}ArO)$_3$mes)$^{4-}$ radical ligand.

Scheme 1. Reaction Scheme[a]

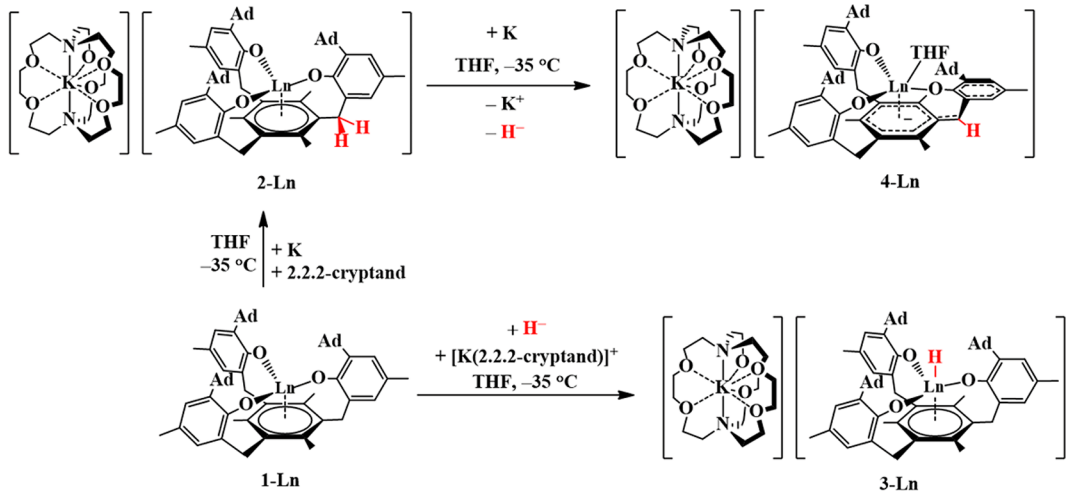

[a]Depicting a possible route to the Ln^{3+} hydride complex [K(2.2.2-cryptand)[((^{Ad,Me}ArO)$_3$mes)LnH], **3-Ln**, and [K(2.2.2-cryptand)][((^{Ad,Me}ArO)$_3$(C$_6$Me$_3$(CH$_2$)$_2$CH))Ln], **4-Ln**, by further reduction of **2-Ln** by potassium.

DOI: 10.1021/acs.inorgchem.8b02053
Inorg. Chem. 2018, 57, 12876−12884

The isolation of [K(2.2.2-cryptand)][((^{Ad,Me}ArO)$_3$($C_6Me_3(CH_2)_2CH$))La], **4-La**, further demonstrates the flexibility of the ((^{Ad,Me}ArOH)$_3$mes)$^{3-}$ ligand and provides the second example of reactivity at the benzylic C−H position. Previously, the U^{4+} hydride complex [((^{Ad,Me}ArO)$_3$-($C_6Me_3(CH_2)_2CH$))U(μ-H)K(Et_2O)], **5-U**, was isolated from reduction reactions involving **1-U** due to C−H bond activation at this position.[12] In **5-U**, one of the benzylic hydrogens is lost as a hydride ligand and binds to U^{4+}. Since lanthanum does not have access to a +4 oxidation state, a lanthanum product analogous to the **5-U** is not possible. Instead, **4-La** contains La^{3+} with a THF ligand in the newly opened coordination site analogous to the position of the hydride in **5-U**. Scheme 1 shows a possible route by which further reduction of **2-Ln** with potassium forms **4-Ln** and a hydride that can react with **1-Ln** to form the observed **3-Ln** products.

CONCLUSION

Reduction of the diamagnetic Y^{3+} complex [((^{Ad,Me}ArO)$_3$mes)-Y], **1-Y**, with potassium generates crystals consisting of two cocrystallized compounds [K(2.2.2-cryptand)][((^{Ad,Me}ArO)$_3$mes)Y]/[K(2.2.2-cryptand)][((^{Ad,Me}ArO)$_3$mes)-YH], **2-Y**/**3-Y**. EPR spectroscopy on complex **2-Y** provides evidence that the ((^{Ad,Me}ArO)$_3$mes)$^{3-}$ ligand is reduced to ((^{Ad,Me}ArO)$_3$mes)$^{4-}$ in this yttrium complex. The hydride ligand in the **3-Y** component of **2-Y**/**3-Y** was definitively identified by NMR spectroscopy. The isolation of a pure crystal of **3-Y** shows that the metrical parameters of the cocrystalline mixtures of the **2-Ln**/**3-Ln** products should be evaluated with caution. The isolation of [K(2.2.2-cryptand)][((^{Ad,Me}ArO)$_3$($C_6Me_3(CH_2)_2CH$))La], **4-La**, demonstrates that the ((^{Ad,Me}ArO)$_3$mes)$^{3-}$ ligand can exhibit C−H bond activation reactivity with rare-earth metals. Therefore, the ((^{Ad,Me}ArO)$_3$mes)$^{3-}$ ligand could be the source of the hydride in the **3-Ln** complexes formed in these reduction reactions. This study establishes the broad flexibility of the ((^{Ad,Me}ArO)$_3$mes)$^{3-}$ ligand: it can support unusual oxidation states, it can be redox-active, and it can provide reactive hydrogen via C−H bond activation.

EXPERIMENTAL DETAILS

The syntheses and manipulations described below were conducted under an argon atmosphere with rigorous exclusion of air and water using glovebox, vacuum line, and Schlenk techniques. Solvents were sparged with ultrahigh purity (UHP) grade argon (Airgas) and passed through columns containing Q-5 and molecular sieves before use. NMR solvents (Cambridge Isotope Laboratories) were dried over NaK/benzophenone, degassed by three freeze−pump−thaw cycles, and vacuum-transferred before use. [$Y(N(SiMe_3)_2)_3$],[20] (^{Ad,Me}ArOH)$_3$mes,[11] and [((^{Ad,Me}ArO)$_3$mes)La][13] were prepared according to their literature procedures. Potassium metal (Aldrich) was washed with hexane and scraped to provide fresh surfaces before use. 2.2.2-Cryptand, 4,7,13,16,21,24-hexaoxa-1,10-diazabicyclo[8.8.8]hexacosane (Acros Organics), was placed under vacuum (1×10^{-3} Torr) for 12 h before use. ^{1}H (500 MHz), ^{13}C (125 MHz, ^{1}H broadband decoupled), and ^{89}Y NMR (25 MHz, ^{1}H broadband decoupled) spectra were obtained on a Bruker GN500 or CRYO500 MHz spectrometer at 298 K. ^{89}Y NMR spectra were referenced using the method described,[53] which is equivalent to referencing $Y(NO_3)_3$ in D_2O. IR samples were prepared as KBr pellets, and the spectra were obtained on either a Varian 1000 or Jasco 4700 FT-IR spectrometer. Elemental analyses were performed on a PerkinElmer 2400 series II CHNS elemental analyzer. EPR spectra were collected using X-band frequency (9.3−9.8 GHz) on a Bruker EMX spectrometer equipped with an ER041XG microwave bridge, and the magnetic field was calibrated with 2,2-diphenyl-1-picrylhydrazyl (DPPH; g = 2.0036). Spectra were simulated with the program W95EPR.[54]

[((^{Ad,Me}ArO)$_3$mes)Y], 1-Y. In an argon-filled glovebox, a sealable 100 mL side-arm Schlenk flask equipped with a greaseless stopcock was charged with a solution of (^{Ad,Me}ArOH)$_3$mes (181 mg, 0.205 mmol) in benzene (40 mL) and a magnetic stir bar. A solution of [$Y(N(SiMe_3)_2)_3$] (123 mg, 0.216 mmol) in benzene (40 mL) was slowly added to the stirred solution. The flask was attached to a Schlenk line, and the mixture was stirred and heated to reflux overnight. The solvent was then removed, and the flask containing the solid mixture was brought back into the glovebox. The resultant colorless solids were washed twice with 10 mL of cold hexane (−35 °C), then dissolved in benzene, and filtered. Toluene (2 mL) was added to the colorless filtrate, and the solvent was removed under vacuum. The colorless gel that resulted was triturated once with hexane to afford **1-Y** as a colorless solid (155 mg, 78%). Colorless single crystals of **1-Y**, suitable for X-ray diffraction, were grown by cooling a concentrated hexane solution to −35 °C. ^{1}H NMR (C_6D_6): δ 7.10 (d, J_{HH} = 2.0 Hz, Ar*H*, 3H), 6.77 (d, J_{HH} = 2.0 Hz, Ar*H*, 3H), 3.73 (s, benzylic CH_2, 6H), 2.41 (s, *Me*, 9H), 2.34 (br s, Ad CH_2, 18H), 2.17 (br s, *Me*, 9H), 1.91 (s, Ad C*H*, 9H), 1.85 (br m, Ad CH_2, 18H). ^{13}C NMR (C_6D_6): δ 158.2, 141.7, 137.7, 136.9, 129.4, 128.6, 126.6, 126.2, 125.8, 41.4, 37.9, 36.6, 29.6, 21.3, 18.9. IR: 3075w, 3033w, 2901s, 2845s, 2727w, 2673w, 2653w, 1604w, 1570w, 1449s, 1413m, 1377m, 1365w, 1355w, 1342m, 1317m, 1305m, 1286m, 1249s, 1208m, 1183m, 1162m, 1148w, 115w, 1101m, 1066w, 1036w, 1016m, 1003w, 980m, 961w, 938w, 923m, 916m, 881m, 858m, 837s, 821s, 810s, 765m, 748m, 741w, 727m, 715m, 702w, 694m, 688w, 677s, 666w, 659w, 653m, 649w, 644w, 640w, 635w, 632w, 627w, 623w, 618w, 614w, 607w, 601w cm^{-1}. Anal. Calcd for $C_{63}H_{75}YO_3$: C, 78.07; H, 7.80. Found: C, 68.41; H, 7.49%. Incomplete combustion resulting in low carbon values was consistently observed in multiple attempts at elemental analysis.

[K(2.2.2-cryptand)][((^{Ad,Me}ArO)$_3$mes)Y]/[K(2.2.2-cryptand)]-[((^{Ad,Me}ArO)$_3$mes)YH], 2-Y/3-Y. In an argon-filled glovebox, a scintillation vial was charged with a THF solution (2 mL) of [(^{Ad,Me}ArO)$_3$mes)Y], **1-Y** (24 mg, 25 μmol), and 2.2.2-cryptand (9 mg, 25 μmol) and the mixture was prechilled in the glovebox freezer (−35 °C). Potassium (excess) was added, and the mixture was stored overnight in the glovebox freezer. The resultant dark red solution was filtered through a prechilled pipet packed with glass wool into a vial containing prechilled Et_2O (8 mL), so that, upon exiting the pipet, the dark red solution was under a layer of Et_2O. The mixture was then stored in the glovebox freezer, and after 48 h, diffusion of Et_2O into the dark red solution yielded dark red single crystals of **2-Y**/**3-Y** suitable for X-ray diffraction (12 mg). Crystallographic modeling was consistent with a 47:53 ratio of **2-Y**/**3-Y**. ^{1}H NMR (THF-d_8): δ 7.81 (d, J_{YH} = 93 Hz, Y−*H*, 1H). The low solubility of the **2-Y**/**3-Y** crystals and the complicated and low-intensity ^{1}H NMR spectrum made it difficult to identify the other resonances. ^{89}Y NMR (THF-d_8): −138.0. IR: 3070w, 2966s, 2899s, 2846s, 2812s, 2760m, 2726m, 2677m, 2653m, 1600w, 1566m, 1477m, 1444s, 1432s, 1418m, 1380m, 1361s, 1354s, 1341m, 1314m, 1307m, 1296s, 1284s, 1277s, 1256s, 1251s, 1210m, 1184m, 1164m, 1134s, 1106s, 1083s, 1071m, 1060m, 1047w, 1033w, 1022w, 1012w, 980m, 949s, 935m, 913m, 904m, 896w, 889w, 878m, 856m, 834m, 817m, 807m, 799m, 785w, 765m, 752m, 749m, 736w, 725w, 719w, 715w, 704w, 699w, 693w, 686w, 676w, 666w, 660w, 653w, 647w, 642w, 629w, 626w, 622w, 615w, 611w, 607w, 603w cm^{-1}. Anal. Calcd for $C_{81}H_{111.55}KN_2O_9Y$: C, 70.23; H, 8.12; N, 2.02. Found: C, 68.33; H, 8.60; N, 1.65 and C, 67.39; H, 8.63; N, 1.68 and C, 67.95; H, 8.24; N, 1.47%. Multiple attempts failed to give satisfactory analysis.

[K(2.2.2-cryptand)][((^{Ad,Me}ArO)$_3$($C_6Me_3(CH_2)_2CH$)La], 4-La. In an argon-filled glovebox, a scintillation vial was charged with **1-La** (48 mg, 47 μmol), 2.2.2-cryptand (18 mg, 47 μmol), and THF (4 mL). To the colorless solution was added excess potassium metal, and the color slowly turned orange. After 16 h at −35 °C, the orange/red mixture was filtered, layered with Et_2O (15 mL), and stored at −35 °C for 48 h, which yielded a mixture of crystals (previously

DOI: 10.1021/acs.inorgchem.8b02053
Inorg. Chem. 2018, 57, 12876−12884

characterized as **2-La**[13]) and a bright orange powder. The powder was washed several times with Et_2O (3 × 10 mL). The residue was dissolved in THF (4 mL), filtered, and layered with hexane (15 mL). Storage at −35 °C for 48 h gave red/orange microcrystalline solids characterized as [K(2.2.2-cryptand)][((^{Ad,Me}ArO)$_3$(C_6Me_3(CH_2)$_2$CH)La(THF)], **4-La**, by X-ray crystallography (15 mg, 21%) (see Supporting Information for crystallographic details). ^{1}H NMR (THF-d_8): 6.60, 6.59, 6.56, 6.54, 6.51, 6.48, 3.96, 3.94, 3.79, 3.70, 3.50, 3.45, 3.18, 3.15, 2.47, 2.24, 2.21, 2.19, 2.17, 2.13 2.12, 2.10, 2.08, 2.03, 2.02, 1.93, 1.59, 1.57, 1.54. IR: 2898s, 2843s, 2725m, 2675m, 2652m, 1600w, 1551m, 1476m, 1444s, 1430m, 1369w, 1360s, 1353s, 1340m, 1314m, 1282s, 1257s, 1238s, 1209w, 1181w, 1173w, 1162w, 1133m, 1105s, 1077m, 1058m, 1027m, 989m, 949, 931m, 913w, 849m, 831m, 818m, 803m, 788w, 769w, 763w, 752m, 739w, 716w, 691w, 682w, 667w, 650w cm^{-1}. Anal. Calcd for $C_{85}H_{118}KLaN_2O_{10}$: C, 67.80; H, 7.90; N, 1.86. Found: C, 66.60; H, 7.73; N, 1.75%. As in the cases above, incomplete combustion perturbed the elemental analysis.

X-ray Data Collection, Structure Determination, and Refinement. Crystallographic details on complexes **1-Y**, **2-Y**/**3-Y**, **3-Y**, and **4-La** are summarized in the Supporting Information.

Computational Details. The initial structures for **2-Y** and **4-La**, obtained from X-ray crystallography, were optimized using the TPSS meta-generalized gradient approximation functional.[52] For all calculations, dispersion corrections were included using the D3 method,[55] and solvation effects were included using the COSMO continuum solvation model.[56] A dielectric constant of 7.52, corresponding to tetrahydrofuran solvent, was used throughout. Numerical integrations were performed using grids of size m5[57] or larger. Basis sets of def2-TZVPP quality were used on the Ln and O, whereas def2-SVP basis sets were used for the remaining atoms.[58] Quasi-relativistic effective potentials were used to model the core electrons of the La atom.[59] For geometry optimizations, an energy convergence criterion of 1 × 10^{-7} au and a gradient convergence of 1 × 10^{-3} au were used. Vibrational analyses were performed to confirm that the optimized structure is a minimum on the potential energy surface. The analyses showed no imaginary modes for **2-Y** and one imaginary mode for **4-La** (47 cm^{-1}) corresponding to the rotations of the methyl group, which are not important to the analysis here. All DFT calculations were performed using the TURBOMOLE 7.2 quantum chemistry package.[60]

■ ASSOCIATED CONTENT

Supporting Information

The Supporting Information is available free of charge on the ACS Publications website at DOI: 10.1021/acs.inorgchem.8b02053.

Additional crystallographic data collection, structure solution and refinement, spectroscopic information, and DFT-optimized structural coordinate modes for **2-Y** and **4-La** (PDF)

Accession Codes

CCDC 1848543−1848547 contain the supplementary crystallographic data for this paper. These data can be obtained free of charge via www.ccdc.cam.ac.uk/data_request/cif, or by emailing data_request@ccdc.cam.ac.uk, or by contacting The Cambridge Crystallographic Data Centre, 12 Union Road, Cambridge CB2 1EZ, UK; fax: +44 1223 336033.

■ AUTHOR INFORMATION

Corresponding Authors

*E-mail: filipp.furche@uci.edu. (F.F.)
*E-mail: karsten.meyer@fau.de. (K.M.)
*E-mail: wevans@uci.edu. (W.J.E.)

ORCID

Chad T. Palumbo: 0000-0001-6436-4602
Dominik P. Halter: 0000-0003-0733-8955
Guo P. Chen: 0000-0002-4743-4450
Filipp Furche: 0000-0001-8520-3971
Karsten Meyer: 0000-0002-7844-2998
William J. Evans: 0000-0002-0651-418X

Notes

The authors declare no competing financial interest.

■ ACKNOWLEDGMENTS

We thank the U.S. National Science Foundation (NSF) for support of the theoretical studies (CHE-1800431 to F.F.) and the experimental studies (CHE-1565776 to W.J.E.). We also thank Prof. A. Rheingold, Dr. C. E. Moore, Dr. J. R. Jones, and M. Wojnar for assistance with X-ray crystallography along with Prof. A. S. Borovik, V. F. Oswald, and Dr. P. R. Dennison for spectroscopic assistance. We also thank NSF for providing graduate fellowship support for C.T.P. (DGE-1321846). D.P.H. acknowledges the Graduate School Molecular Science (GSMS) of FAU Erlangen-Nürnberg for the generous support. The Bundesministerium für Bildung und Forschung (BMBF, support codes 02NUK012C and 02NUK020C), the FAU Erlangen-Nürnberg, and COST Action CM1006 are acknowledged for funding.

■ REFERENCES

(1) Hitchcock, P. B.; Lappert, M. F.; Maron, L.; Protchenko, A. V. Lanthanum Does Form Stable Molecular Compounds in the +2 Oxidation State. *Angew. Chem., Int. Ed.* **2008**, *47* (8), 1488−149.

(2) MacDonald, M. R.; Bates, J. E.; Ziller, J. W.; Furche, F.; Evans, W. J. Completing the Series of +2 Ions for the Lanthanide Elements: Synthesis of Molecular Complexes of Pr^{2+}, Gd^{2+}, Tb^{2+}, and Lu^{2+}. *J. Am. Chem. Soc.* **2013**, *135* (26), 9857−9868.

(3) Fieser, M. E.; MacDonald, M. R.; Krull, B. T.; Bates, J. E.; Ziller, J. W.; Furche, F.; Evans, W. J. Structural, Spectroscopic, and Theoretical Comparison of Traditional vs Recently Discovered Ln^{2+} Ions in the [K(2.2.2-cryptand)][($C_5H_4SiMe_3$)$_3$Ln] Complexes: The Variable Nature of Dy^{2+} and Nd^{2+}. *J. Am. Chem. Soc.* **2015**, *137* (1), 369−382.

(4) MacDonald, M. R.; Fieser, M. E.; Bates, J. E.; Ziller, J. W.; Furche, F.; Evans, W. J. Identification of the +2 Oxidation State for Uranium in a Crystalline Molecular Complex, [K(2.2.2-cryptand)][($C_5H_4SiMe_3$)$_3$U]. *J. Am. Chem. Soc.* **2013**, *135* (36), 13310−13313.

(5) Langeslay, R. R.; Fieser, M. E.; Ziller, J. W.; Furche, F.; Evans, W. J. Synthesis, Structure, and Reactivity of Crystalline Molecular Complexes of the {[C_5H_3($SiMe_3$)$_2$]$_3$Th}$^{1-}$ Anion Containing Thorium in the Formal +2 Oxidation State. *Chem. Sci.* **2015**, *6* (1), 517−521.

(6) Windorff, C. J.; MacDonald, M. R.; Meihaus, M. R.; Ziller, J. W.; Long, J. R.; Evans, W. J. Expanding the Chemistry of Molecular U^{2+} Complexes: Synthesis, Characterization, and Reactivity of the {[C_5H_3($SiMe_3$)$_2$]$_3$U}$^-$ Anion. *Chem. - Eur. J.* **2016**, *22* (2), 772−782.

(7) Windorff, C. J.; Chen, G. P.; Cross, J. N.; Evans, W. J.; Furche, F.; Gaunt, A. J.; Janicke, M. T.; Kozimor, S. A.; Scott, B. L. Identification of the Formal +2 Oxidation State of Plutonium: Synthesis and Characterization of {Pu^{II}[C_5H_3($SiMe_3$)$_2$]$_3$}$^-$. *J. Am. Chem. Soc.* **2017**, *139* (11), 3970−3973.

(8) Su, J.; Windorff, C. J.; Batista, E. R.; Evans, W. J.; Gaunt, A. J.; Janicke, M. T.; Kozimor, S. A.; Scott, B. L.; Woen, D. H.; Yang, P. Identification of the Formal +2 Oxidation State of Neptunium: Synthesis and Structural Characterization of {Np^{II}[C_5H_3($SiMe_3$)$_2$]$_3$}$^{1-}$. *J. Am. Chem. Soc.* **2018**, *140* (24), 7425−7428.

(9) Evans, W. J. Tutorial on the Role of Cyclopentadienyl Ligands in the Discovery of Molecular Complexes of the Rare-Earth and Actinide Metals in New Oxidation States. *Organometallics* **2016**, *35* (18), 3088−3100.

DOI: 10.1021/acs.inorgchem.8b02053
Inorg. Chem. 2018, 57, 12876−12884

(10) Woen, D. H.; Evans, W. J. In *Handbook on the Physics and Chemistry of Rare Earths,* 1st ed.; Elsevier: Amsterdam, Netherlands, 2016; Vol. *50*, pp 337−394.
(11) La Pierre, H. S.; Scheurer, A.; Heinemann, F. W.; Hieringer, W.; Meyer, K. Synthesis and Characterization of a Uranium(II) Monoarene Complex Supported by d Backbonding. *Angew. Chem., Int. Ed.* **2014**, *53* (28), 7158−7162.
(12) La Pierre, H. S.; Kameo, H.; Halter, D. P.; Heinemann, F. W.; Meyer, K. Coordination and Redox Isomerization in the Reduction of a Uranium(III) Monoarene Complex. *Angew. Chem., Int. Ed.* **2014**, *53* (28), 7154−7157.
(13) Fieser, M. E.; Palumbo, C. T.; La Pierre, H. S.; Halter, D. P.; Voora, V.; Ziller, J. W.; Furche, F.; Meyer, K.; Evans, W. J. Comparisons of Lanthanide/Actinide +2 Ions in a Tris(aryloxide)-arene Coordination Environment. *Chem. Sci.* **2017**, *8* (11), 7424−7433.
(14) Palumbo, C. T.; Halter, D. P.; Voora, V. K.; Chen, G. P.; Chan, A. K.; Fieser, M. E.; Ziller, J. W.; Hieringer, W.; Furche, F.; Meyer, K.; Evans, W. J. Metal versus Ligand Reduction in Ln^{3+} Complexes of a Mesitylene-Anchored Tris(Aryloxide) Ligand. *Inorg. Chem.* **2018**, *57* (5), 2823−2833.
(15) Cassani, M. C.; Duncalf, D. J.; Lappert, M. F. The First Example of a Crystalline Subvalent Organolanthanum Complex: [K([18]crown-6)- $(\eta^2\text{-}C_6H_6)_2$][$(LaCp^{tt}_2)_2(\mu\text{-}\eta^6\text{:}\eta^6\text{-}C_6H_6)$]•$2C_6H_6$ (Cp^{tt}) $\eta^5\text{-}C_5H_3Bu^t_2$-1,3). *J. Am. Chem. Soc.* **1998**, *120* (49), 12958−12959.
(16) Jaroschik, F.; Nief, F.; Le Goff, X. F.; Ricard, L. Isolation of Stable Organomdysprosium(II) Complexes by Chemical Reduction of Dysprosium(III) Precursors. *Organometallics* **2007**, *26* (5), 1123−1125.
(17) Jaroschik, F.; Momin, A.; Nief, F.; Le Goff, X. F.; Deacon, G. B.; Junk, P. C. Dinitrogen Reduction and C−H Activation by the Divalent Organoneodymium Complex [$(C_5H_2tBu_3)_2$Nd(μ-I)K([18]-crown-6)]. *Angew. Chem.* **2009**, *121* (6), 1137−1141.
(18) Holton, J.; Lappert, M. F.; Ballard, D. G. H.; Pearce, R.; Atwood, D. A.; Hunter, W. E. Dimeric μ-Dimethyl Lanthanide Complexes, a New Class of Electron-deficient Compound, and the Crystal and Molecular Structure of $[Yb(\eta\text{-}C_5H_5)_2Me]_2$. *J. Chem. Soc., Chem. Commun.* **1976**, 480−481.
(19) Schumann, H.; Meese-Marktscheffel, J. A.; Esser, L. Synthesis, Structure, and Reactivity of Organometallic π-Complexes of the Rare Earths in the Oxidation State Ln^{3+} with Aromatic Ligands. *Chem. Rev.* **1995**, *95* (4), 865−986.
(20) Bradley, D. C.; Ghotra, J. S.; Hart, F. A. Low Co-ordination Numbers in Lanthanide and Actinide Compounds. Part I. Preparation and Characterization of Tris{bis(trimethylsilyl)amide}lanthanides. *J. Chem. Soc., Dalton Trans.* **1973**, 1021−1023.
(21) Shannon, R. D. Revised Effective Ionic-Radii and Systematic Studies of Interatomic Distances in Halides and Chalcogenides. *Acta Crystallogr., Sect. A: Cryst. Phys., Diffr., Theor. Gen. Crystallogr.* **1976**, *32* (5), 751−767.
(22) Takenaka, Y.; Hou, Z. Lanthanide Terminal Hydride Complexes Bearing Two Sterically Demanding $C_5Me_4SiMe_3$ Ligands. Synthesis, Structure, and Reactivity. *Organometallics* **2009**, *28* (17), 5196−5203.
(23) Den Haan, K. H.; Wielstra, Y.; Teuben, J. H. Reactions of Yttrium-Carbon Bonds with Active Hydrogen-Containing Molecules. A Useful Synthetic Method for Permethylyttrocene Derivatives. *Organometallics* **1987**, *6* (10), 2053−2060.
(24) Gavenonis, J.; Tilley, T. D. Synthesis and Reactivity of Bis(heptamethylindenyl) Yttrium (Ind^*_2Y) Complexes Containing Alkyl and Hydride Ligands: Crystal Structure of $Ind^*_2YCl(THF)$. *J. Organomet. Chem.* **2004**, *689* (4), 870−878.
(25) Arndt, S.; Kramer, M. U.; Fegler, W.; Nakajima, Y.; Del Rosal, I.; Poteau, R.; Spaniol, T. P.; Maron, L.; Okuda, J. Yttrium Dihydride Cation $[YH_2(THF)_2]^{+n}$: Aggregate Formation and Reaction with (NNNN)-Type Macrocycles. *Organometallics* **2015**, *34* (15), 3739−3747.
(26) Hultzsch, K. C.; Voth, P.; Beckerle, K.; Spaniol, T. P.; Okuda, J. Single-Component Polymerization Catalysts for Ethylene and Styrene: Synthesis, Characterization, and Reactivity of Alkyl and Hydrido Yttrium Complexes Containing a Linked Amido−Cyclopentadienyl Ligand. *Organometallics* **2000**, *19* (3), 228−243.
(27) Evans, W. J.; Meadows, J. H.; Wayda, A. L.; Hunter, W. E.; Atwood, J. L. Organolanthanide Hydride Chemistry. 1. Synthesis and X-ray Crystallographic Characterization of Dimeric Organolanthanide and Organoyttrium Hydride Complexes. *J. Am. Chem. Soc.* **1982**, *104* (7), 2008−2014.
(28) Evans, W. J.; Drummond, D. K.; Hanusa, T. P.; Doedens, R. J. Bis(1,3-dimethylcyclopentadienyl) Yttrium Complexes. Synthesis and X-ray Crystallographic Characterization of $[1,3\text{-}Me_2C_5H_3)_2Y(\mu\text{-}Me)]_2$, $[1,3\text{-}Me_2C_5H_3)_2Y(\mu\text{-}H)]_3$, and $[1,3\text{-}Me_2C_5H_3)_2(THF)Y(\mu\text{-}H)]_2$. *Organometallics* **1987**, *6* (11), 2279−2285.
(29) Voskoboynikov, A. Z.; Parshina, I. N.; Shestakova, A. K.; Butin, K. P.; Beletskaya, I. P.; Kuz'mina, L. G.; Howard, J. A. K. Reactivity of Lanthanide and Yttrium Hydrides and Hydrocarbyls toward Organosilicon Hydrides and Related Compounds. *Organometallics* **1997**, *16* (19), 4041−4055.
(30) Kretschmer, W. P.; Troyanov, S. I.; Meetsma, A.; Hessen, B.; Teuben, J. H. Regioselective Homo- and Codimerization and α-Olefins Catalyzed by Bis(2,4,7-trimethylindenyl)yttrium Hydride. *Organometallics* **1998**, *17* (3), 284−286.
(31) Deng, D.; Jiang, Y.; Qian, C.; Wu, G.; Zheng, P. L., XIII Synthesis, Spectroscopic and X-ray Crystallographic Characterization of New Early Organolanthanide, and Organoholmium Hydroxide Complexes. *J. Organomet. Chem.* **1994**, *470* (1−2), 99−107.
(32) Ye, C.; Qian, C.; Yang, X. Studies on Organolanthanide Complexes: XXXV. Synthesis and Reactivity of New Organo Rare Earth Hydrides. *J. Organomet. Chem.* **1991**, *407* (3), 329−335.
(33) Coughlin, E. B.; Bercaw, J. E. Iso-specific Ziegler-Natta Polymerization of α-olefins with a Single-Component Organoyttrium Catalyst. *J. Am. Chem. Soc.* **1992**, *114* (19), 7606−7607.
(34) Mitchell, J. P.; Hajela, S.; Brookhart, S. K.; Hardcastle, K. I.; Henling, L. M.; Bercaw, J. E. Preparation and Structural Characterization of an Enantiomerically Pure, C2-Symmetric, Single-Component Ziegler−Natta α-Olefin Polymerization Catalyst. *J. Am. Chem. Soc.* **1996**, *118* (5), 1045−1053.
(35) Giardello, M. A.; Conticello, V. P.; Brard, L.; Sabat, M.; Rheingold, A. L.; Stern, C. L.; Marks, T. J. Chiral Organolanthanides Designed for Asymmetric Catalysis. Synthesis, Characterization, and Configurational Interconversions of Chiral, C_1-Symmetric Organolanthanide Halides, Amides, and Hydrocarbyls. *J. Am. Chem. Soc.* **1994**, *116* (22), 10212−10240.
(36) Stern, D.; Sabat, M.; Marks, T. J. Manipulation of Organolanthanide Coordinative Unsaturation. Synthesis, Structures, Structural Dynamics, Comparative Reactivity, and Comparative Thermochemistry of Dinuclear μ-hydrides and μ-alkyls with $[\mu\text{-}R_2Si(Me_4C_5)(C_5H_4)]_2$ Supporting Ligation. *J. Am. Chem. Soc.* **1990**, *112* (26), 9558−9575.
(37) Coughlin, E. B.; Henling, L. M.; Bercaw, J. E. Synthesis and Structural Characterization of $[(\eta^5\text{-}C_5Me_4)_5SiMe_2]YCH(SiMe_3)_2$. Hydrogenation to $[[(\eta^5\text{-}C_5Me_4)_2SiMe_2]Y]_2(\mu_2\text{-}H)_2$ and its Facile Ligand Redistribution to $Y_2[\mu_2\text{-}[(\eta^5\text{-}C_5Me_4)SiMe_2(\eta^5\text{-}C_5Me_4)]]_2(\mu_2\text{-}H)_2$. *Inorg. Chim. Acta* **1996**, *242* (1−2), 205−210.
(38) Schaverien, C. J. Alkoxides as Ancillary Ligands in Organolanthanide Chemistry: Synthesis of, Reactivity of, and Olefin Polymerization by the μ-Hydride-μ-Alkyl Compounds $[Y(C_5Me_5)(OC_6H_3{}^tBu_2)]_2(\mu\text{-}H)(\mu\text{-alkyl})$. *Organometallics* **1994**, *13* (1), 69−82.
(39) Schaverien, C. J. Organometallic Chemistry of the Lanthanides. In *Advances in Organometallic Chemistry;* Stone, F. G. A., West, R., Eds.; Academic Press Inc: San Diego, CA, 1994, Vol. *36*, pp 283−362.
(40) Duchateau, R.; van Wee, C. T.; Meetsma, A.; van Duijnen, P. T.; Teuben, J. H. Ancillary Ligand Effects in Organoyttrium Chemistry: Synthesis, Characterization, and Electronic Structure of Bis(benzamidinato)yttrium Compounds. *Organometallics* **1996**, *15* (9), 2279−2290.

DOI: 10.1021/acs.inorgchem.8b02053
Inorg. Chem. 2018, 57, 12876−12884

(41) Trifonov, A. A.; Spaniol, T. P.; Okuda, J. Yttrium Hydrido Complexes that Contain a Less "Constrained Geometry" Ligand: Synthesis, Structure, and Efficient Hydrosilylation Catalysis. *Organometallics* **2001**, *20* (23), 4869−4874.
(42) Evans, W. J.; Meadows, J. H.; Kostka, A. G.; Closs, G. L. Yttrium-89 NMR Spectra of Organoyttrium Complexes. *Organometallics* **1985**, *4* (2), 324−326.
(43) Long, D. P.; Bianconi, P. A. A Catalytic System for Ethylene Polymerization Based on Group III and Lanthanide Complexes of Tris(pyrazolyl)borate Ligands. *J. Am. Chem. Soc.* **1996**, *118* (49), 12453−12454.
(44) Evans, W. J.; Meadows, J. H.; Hanusa, T. P. Organolanthanide and Organoyttrium Hydride Chemistry. 6. Direct Synthesis and ^{1}H NMR Spectral Analysis of the Trimetallic Yttrium and Yttrium-Zirconium Tetrahydride Complexes, $\{[(C_5H_5)_2YH]_3H\}\{Li(THF)_4\}$ and $\{[(CH_3C_5H_4)_2YH]_2[(CH_3C_5H_4)_2ZrH]H]$. *J. Am. Chem. Soc.* **1984**, *106* (16), 4454−4460.
(45) Evans, W. J.; Sollberger, M. S.; Khan, S. I.; Bau, R. Reactivity of Trimetallic Organoyttrium Hydride Complexes. Synthesis of the Alkoxy Hydride Anions $[[(C_5H_5)_2Y(\mu\text{-}H)]_x[(C_5H_5)_2Y(\mu\text{-}OCH_3)]_{3-x}(\mu_3\text{-}H)]^-$ (x = 0−2), Including the X-ray Crystal Structure of $[[(C_5H_5)_2Y(\mu\text{-}OCH_3)]_3(\mu_3\text{-}H)]_2[Li(THF)_3]_2$. *J. Am. Chem. Soc.* **1988**, *110* (2), 439−446.
(46) Hultzsch, K. C.; Voth, P.; Spaniol, T. P.; Okuda, J. Synthese und Charakterisierung eines vierkernigen Hydrid-Clusters von Yttrium $[\{\eta^5\text{-}(C_5Me_4SiMe_3)Y\}_4(\mu\text{-}H)_4(\mu_3\text{-}H)_4(THF)_2]$. *Z. Anorg. Allg. Chem.* **2003**, *629* (7−8), 1272−1276.
(47) Piper, T. S.; Wilkinson, G. Alkyl and Aryl Derivatives of π-Cyclopentadienyl Compounds of Chromium, Molybdenum, Tungesten, and Iron. *J. Inorg. Nucl. Chem.* **1956**, *3* (2), 104−124.
(48) Corbey, J. F.; Woen, D. H.; Palumbo, C. T.; Fieser, M. E.; Ziller, J. W.; Furche, F.; Evans, W. J. Ligand Effects in the Synthesis of Ln^{2+} Complexes by Reduction of Tris(cyclopentadienyl) Precursors including C−H bond Activation of an Indenyl Anion. *Organometallics* **2015**, *34* (15), 3909−3921.
(49) MacDonald, M. R.; Ziller, J. W.; Evans, W. J. Synthesis of a Crystalline Molecular Complex of Y^{2+}, $[(18\text{-crown-}6)K]\text{-}[(C_5H_4SiMe_3)_3Y]$. *J. Am. Chem. Soc.* **2011**, *133* (40), 15914−159147.
(50) Huh, D. N.; Darago, L. E.; Ziller, J. W.; Evans, W. J. Utility of Lithium in Rare-Earth Metal Reduction Reactions to Form Nontraditional Ln^{2+} Complexes and Unusual $[Li(2.2.2\text{-cryptand})]^{1+}$ Cations. *Inorg. Chem.* **2018**, *57* (4), 2096−2102.
(51) Fang, M.; Lee, D. S.; Ziller, J. W.; Doedens, R. J.; Bates, J. E.; Furche, F.; Evans, W. J. Synthesis of the $(N_2)^{3-}$ Radical from Y^{2+} and Its Protonolysis Reactivity To Form $(N_2H_2)^{2-}$ via the $Y[N(SiMe_3)_2]_3/KC_8$ Reduction System. *J. Am. Chem. Soc.* **2011**, *133* (11), 3784−3787.
(52) Tao, J.; Perdew, J. P.; Staroverov, V. N.; Scuseria, G. E. Climbing the Density Functional Ladder: Nonempirical Meta-Generalized Gradient Approximation Designed for Molecules and Solids. *Phys. Rev. Lett.* **2003**, *91* (14), 146401.
(53) Harris, R. K.; Becker, E. D.; Cabral de Menezes, S. M.; Granger, P.; Hoffman, R. E.; Zilm, K. W. Further Conventions for NMR Shielding and Chemical Shifts. *Pure Appl. Chem.* **2008**, *80* (1), 59−84.
(54) Neese, F. Ph.D. Thesis, University of Konstanz, 1993.
(55) Grimme, S.; Antony, J.; Ehrlich, S.; Krieg, S. A Consistent and Accurate *ab initio* Parametrization of Density Functional Dispersion Correction (DFT-D) for the 94 Elements H-Pu. *J. Chem. Phys.* **2010**, *132* (15), 154104.
(56) Klamt, A.; Schüürmann, G. J. COSMO: A New Approach to Dielectric Screening in Solvents with Explicit Expressions for the Screening Energy and its Gradient. *J. Chem. Soc., Perkin Trans. 2* **1993**, *2*, 799−805.
(57) Treutler, O.; Ahlrichs, R. Efficient Molecular Numerical Integration Schemes. *J. Chem. Phys.* **1995**, *102* (1), 346−354.
(58) Weigend, F.; Ahlrichs, R. Balanced Basis Sets of Split Valence, Triple Zeta Valence and Quadruple Zeta Valence Quality for H to Rn: Design and Assessment of Accuracy. *Phys. Chem. Chem. Phys.* **2005**, *7* (18), 3297−3305.
(59) Dolg, M.; Stoll, H.; Savin, A.; Preuss, H. Energy-adjusted pseudopotentials for the rare earth elements. *Theor. Chim. Acta.* **1989**, *75* (3), 173.
(60) Furche, F.; Ahlrichs, R.; Hättig, C.; Klopper, W.; Sierka, M.; Weigend, F. Turbomole. *WIREs Comput. Mol. Sci.* **2014**, *4* (2), 91−100.

DOI: 10.1021/acs.inorgchem.8b02053
Inorg. Chem. 2018, 57, 12876−12884